

Sex-ratio bias induced by mutation

Minjae Kim,¹ Hyeong-Chai Jeong,² and Seung Ki Baek^{1,*}

¹*Department of Physics, Pukyong National University, Busan 48513, Korea*

²*Department of Physics and Astronomy,
Sejong University, Seoul 05006, Korea*

Abstract

A question in evolutionary biology is why the number of males is approximately equal to that of females in many species, and Fisher's theory of equal investment answers that it is the evolutionarily stable state. The Fisherian mechanism can be given a concrete form by a genetic model based on the following assumptions: (1) Males and females mate at random. (2) An allele acts on the father to determine the expected progeny sex ratio. (3) The offspring inherits the allele from either side of the parents with equal probability. The model is known to achieve the 1:1 sex ratio due to the invasion of mutant alleles with different progeny sex ratios. In this study, however, we argue that mutation plays a more subtle role in that fluctuations caused by mutation renormalize the sex ratio and thereby keep it away from 1 : 1 in general. This finding shows how the sex ratio is affected by mutation in a systematic way, whereby the effective mutation rate can be estimated from an observed sex ratio.

PACS numbers: 05.10.Cc,87.23.Kg

* seungki@pknu.ac.kr

I. INTRODUCTION

The number of males per female is close to one in the world population, and the value has been found stable across many countries [1]. This 1:1 sex ratio at birth is also commonly observed in many other sexually reproducing species. This is indeed highly nontrivial in that the ratio is suboptimal from the viewpoint of the population: As far as the growth rate is concerned, which is directly related to reproductive success of the species, it would be more efficient to produce more females than males because females can give birth to offspring. This female-biased state cannot be sustained, however, and the reason can be understood from the “selfish-gene” point of view. Along this line, Fisher’s theory states that the one-to-one ratio between males and females is the evolutionarily stable state in this game of genes [2]. The argument goes as follows [3]: Consider an individual with n offspring, of which nx are male and the others are female ($0 \leq x \leq 1$). This individual’s next generation has K offspring in total, where KX and $K(1 - X)$ are the numbers of males and females, respectively ($0 < X < 1$). In this case, the relative investment of the individual is $C_{\text{inv}} = n/(2K)$ because we assume that an offspring inherits one half of the genes from either parent. The focal individual’s genetic contribution to the population is $C_1 = C_{\text{inv}}$, which is a reference point to judge an individual’s genetic success. The situation becomes different in the second next generation: If males and females mate randomly, then the focal individual’s genetic contribution is calculated as

$$C_2 = \frac{1}{4} \left(\frac{nx}{KX} + \frac{n\tilde{x}}{K\tilde{X}} \right), \quad (1)$$

where $\tilde{x} \equiv 1 - x$ and $\tilde{X} \equiv 1 - X$. According to this formula, if X exceeds $1/2$, then C_2 is greater than C_{inv} for $x < X$. By symmetry, it is also obvious that $C_2 > C_{\text{inv}}$ for $x > X$ if X is less than $1/2$. It thus follows that it is genetically beneficial to “invest” in the rare sex, which constitutes the basic mechanism for maintaining the Fisherian sex ratio of 1:1. In this sense, the sex-ratio problem is an example of conflict between individual and collective interests [4].

The Fisherian mechanism has many subtleties, and still not much is known about deviations from its prediction [5, 6]. In particular, it is noteworthy that if the population achieves this predicted ratio, i.e., $X = 1/2$, C_2 of Eq. (1) becomes C_{inv} regardless of an individual’s x as long as the population size is large enough [7]. It implies that the timescale of this

evolutionary dynamics may actually diverge as the restoring force toward $X = 1/2$ vanishes at this point. Put differently, if mutation occurs with a rate μ , the timescale would be of an order of μ^{-1} , and Fisher's ratio $X = 1/2$ can be achieved in a limit of $\mu \rightarrow 0$. If μ is small yet finite, on the other hand, the 1:1 ratio may not be reached within finite time.

In this work, we show that a dynamic equilibrium out of 1:1 actually forms in a minimal model devised for Fisher's theory. This is counterintuitive because mutation is an essential ingredient of the Fisherian mechanism. In short, it cannot work without mutation, and it cannot work with it either. We will explain this observation in the following way: In the next section, we introduce a genetic model and study it with three different approaches: Monte Carlo simulation, integrodifference equations, and renormalization analysis. We discuss the implications in Sec. III and then conclude this work in Sec. IV.

II. GENETIC MODEL

A. Monte Carlo simulation

Although Eq. (1) illustrates the basic mechanism of Fisher's theory, a more detailed view is provided by genetic models [8–10], of which we will investigate the simplest one called a haploid model [11]. As a Monte Carlo version of it, let us consider a population of N individuals with the following assumptions: (i) Every individual i has two attributes, i.e., one is the allele related with the expected progeny ratio denoted by x_i , and the other is the sex. (ii) For each mating event, we randomly choose a male and a female as parents. (iii) The resulting offspring inherits either x_{father} or x_{mother} equally probably, and (iv) the sex is male with probability x_{father} . (v) With probability $\mu \ll 1$, mutation changes x_i to a random number drawn from a probability density function on the unit interval, which we choose to be the uniform distribution $\mathcal{U}(0, 1)$ for the sake of analytic tractability. (vi) One generation consists of N mating events to produce N individuals of the offspring generation, and an individual may be chosen to mate more than once. This is a model of nonoverlapping generations in the sense that the offspring generation completely replaces the parental one, which is common in many evolutionary models.

The first three assumptions are already found in the evolutionary-stability argument [see, e.g., Eq. (1)]. On the other hand, we adopt from Ref. 11 the fourth assumption that only one

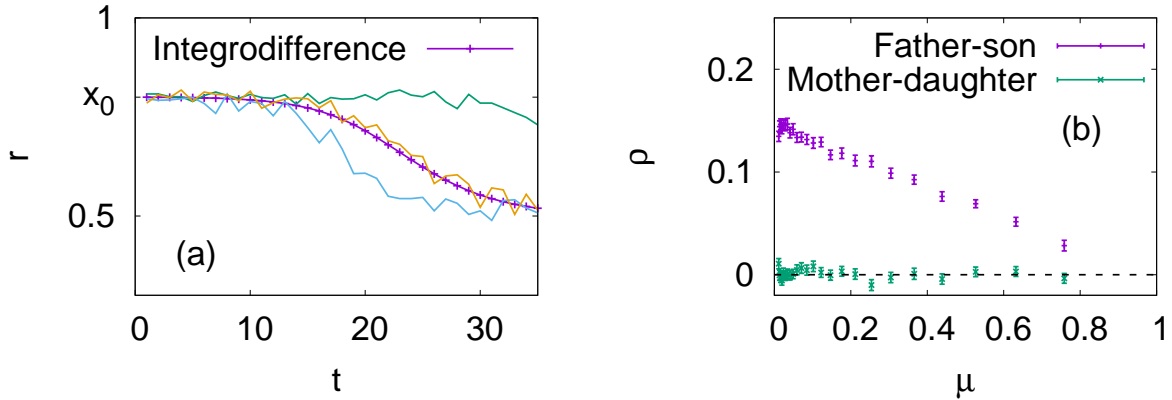


FIG. 1. (Color online) (a) Time evolution of the male fraction with $\mu = 10^{-3}$. The horizontal axis represents time in units of generations. Initially, every individual has an equal expected progeny sex ratio, $x_0 = 0.8$, and the numbers of males and females are the same. The lines are obtained from Monte Carlo calculation with population size $N = 10^3$, and the linepoints are from the integrodifference equations [Eqs. (4) and (5)] started with $\phi^m(x, t = 0) = \phi^f(x, t = 0) = \delta(x - x_0)/2$. (b) Pearson correlation coefficient of the offspring sex ratio between parents and children, calculated from the Monte Carlo simulation for various values of μ . The population size is $N = 10^3$, and we have used 10^2 equilibrated samples. The offspring sex ratio of a father is positively correlated with that of his sons who have offspring, and the degree of correlation decreases as μ grows. No such correlation exists between mothers and daughters.

parent's allele is relevant to the expected progeny sex ratio. Yet the difference from Ref. 11 is that we regard the father as the relevant side, which has been supported by empirical studies [12–14]. Note that this is the point where the symmetry between males and females is broken. Most importantly, it is purely hypothetical that the expected progeny sex ratio is determined by a single gene as in this model (see, however, Ref. 14 for more discussion). With regard to the fifth assumption, such memoryless mutation with full variation within the unit interval would certainly be ideal, but we can always think of an effective mutation rate with which the genetic information is lost. We will see below that the choice of the uniform distribution greatly simplifies our analysis in calculating the average effect of mutation.

A typical simulation result is shown in Fig. 1(a), where one can see the average fraction of males, denoted by r , approach $1/2$ as time t goes by, even if the system starts from a state far from $x = 1/2$. However, if one measures the average carefully, $r(t \rightarrow \infty)$ is actually

slightly above $1/2$, as will be detailed below. Before proceeding, we stress that this Monte Carlo approach provides detailed information of the population. For example, we can trace the offspring sex ratio of a father and compare it with that of his son. The correlation in their offspring sex ratios can thus be calculated as a function of μ [Fig. 1(b)]. The ratios are positively correlated between fathers and sons, whereas they are not between mothers and daughters, in accordance with Ref. 14.

B. Integrodifference equations

To observe this deviation without statistical fluctuations, let us deal with an infinite population. We define $\phi^m(x, t)dx$ as the probability of being male with an expected progeny sex ratio $\in (x, x + dx)$ at generation t . The fraction of males in the total population will thus be $r(t) = \int_0^1 \phi^m(x, t)dx$. We define $\phi^f(x, t)$ as the female counterpart, together with the fraction of females, $\int_0^1 \phi^f(x, t)dx = 1 - r(t)$. According to the population dynamics given above, the time evolution is described by the following integrodifference equations in the absence of mutation:

$$\phi_{\mu=0}^m(x, t+1) = \frac{1}{2} \left[\frac{\phi^m(x, t)}{r(t)}x + \frac{\phi^f(x, t)}{1-r(t)} \langle x \rangle_m \right] \quad (2)$$

$$\phi_{\mu=0}^f(x, t+1) = \frac{1}{2} \left[\frac{\phi^m(x, t)}{r(t)}\tilde{x} + \frac{\phi^f(x, t)}{1-r(t)} \langle \tilde{x} \rangle_m \right], \quad (3)$$

where $\langle x \rangle_m \equiv \int_0^1 x\phi^m(x, t)/r(t)dx$ and $\langle \tilde{x} \rangle_m \equiv 1 - \langle x \rangle_m$. When mutation happens to individuals randomly drawn without replacement, the full dynamics can be written as

$$\phi^m(x, t+1) = (1 - \mu)\phi_{\mu=0}^m(x, t+1) + \mu \langle x \rangle_m \quad (4)$$

$$\phi^f(x, t+1) = (1 - \mu)\phi_{\mu=0}^f(x, t+1) + \mu \langle \tilde{x} \rangle_m, \quad (5)$$

where μ is the mutation rate. The right-hand sides of Eqs. (4) and (5) are determined by $\phi_{\mu=0}^m$ and $\phi_{\mu=0}^f$ at t , as one can see by plugging Eqs. (2) and (3) there. Note that if one integrates Eq. (4) over x , with ϕ_0^m given in Eq. (2), it correctly leads to $r(t+1) = \langle x \rangle_m$, confirming that fathers determine the progeny sex ratio. If we start from uniform distribution $\phi^m(x, t=0) = \phi^f(x, t=0) = 1/2$, then numerical iteration of Eqs. (4) and (5) shows that $r(t)$ converges to a stationary value away from $1/2$ as $t \rightarrow \infty$ [Fig. 2(a)]. The stationary sex ratio is well fitted by the least-squares method to

$$r_{\infty}^{\text{fit}}(\mu) \approx 1/2 + 0.5\mu - 2.8\mu^2. \quad (6)$$

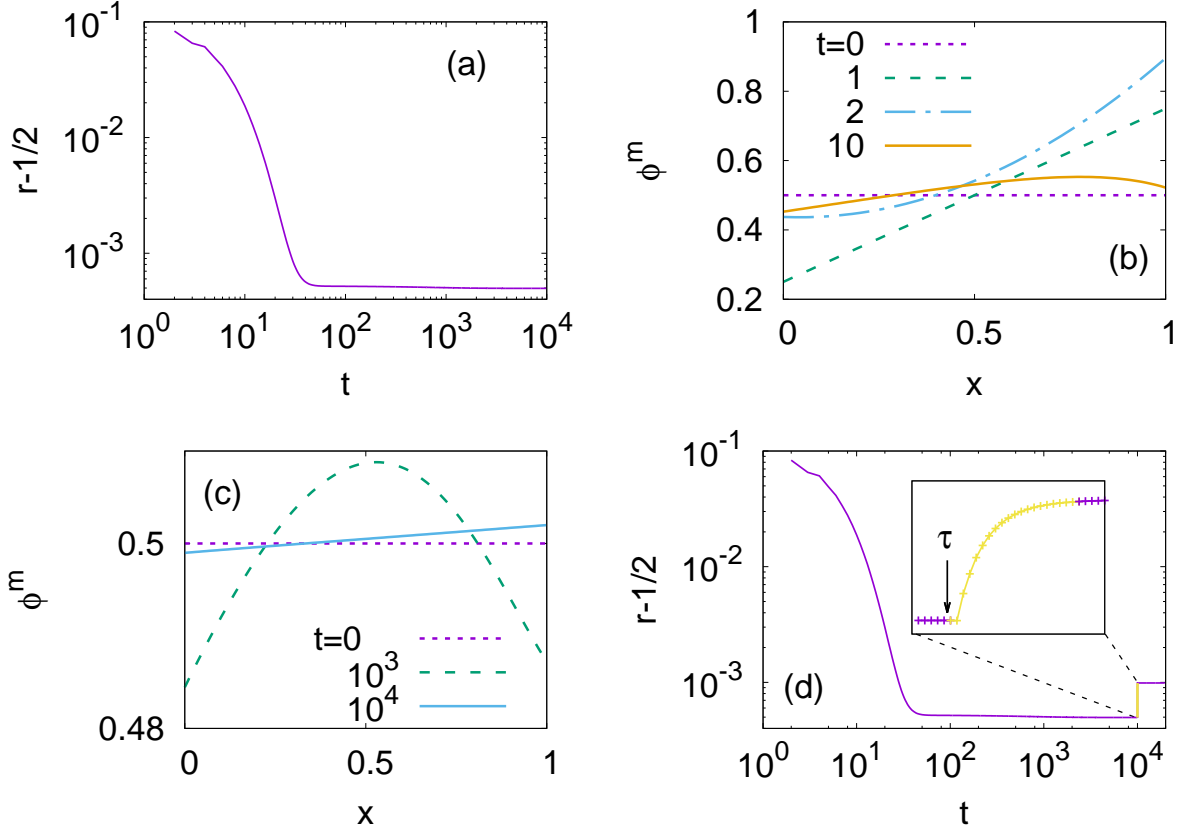


FIG. 2. (Color online) (a) The sex ratio deviation from $1/2$, obtained by iterating Eqs. (4) and (5). The initial condition is given as $\phi^m(x, t = 0) = \phi^f(x, t = 0) = 1/2$. Note that $r(t = 1)$ is exactly $1/2$ for this initial condition because $r(t + 1) = \langle x \rangle_m$. We use the trapezoidal rule [15] in evaluating integrals such as $r(t)$ and $\langle x \rangle_m$. (b) Short-time and (c) long-time evolution of $\phi^m(x, t)$ from the same uniform random initial condition as in (a). (d) Transition to another stationary state when μ changes to $\mu' = 2\mu$ immediately after time $\tau = 10^4$. Inset: Zoomed view around $t = \tau$, where the first 20 generations after the change are drawn in light yellow.

It is also instructive to look into $\phi^m(x, t)$ itself: At $t \lesssim O(10)$, individuals with larger x occupy higher portions in $\phi^m(x, t)$ because they are more likely to produce male offspring [Fig. 2(b)]. This effect competes with the loss of genetic contribution in the Fisherian mechanism, generating a unimodal shape at $t \sim O(10)$. These two effects eventually balance each other by making $\phi^m(x, t)$ a linear function of x with a small positive slope [Fig. 2(c)]. In Appendix A, we show how one can find the functional forms of the stationary distributions ϕ_{st}^m and ϕ_{st}^f as Taylor series. Although it takes long from the uniform initial condition to this stationary state, the distance between stationary states of different μ 's is relatively short

TABLE I. Frequencies and the progeny types of the four mating cases in the haploid model with two alleles a and A . A male with the mutant allele a will have a son with probability x , whereas the probability is X for a male with the resident allele A . We have defined $\tilde{X} \equiv 1 - X$ and $\tilde{x} \equiv 1 - x$.

| $\sigma \times \varphi$ | frequency | daughters | | sons | |
|-------------------------|----------------------|------------------------|------------------------|----------------|----------------|
| | | a | A | a | A |
| $a \times a$ | $q_m q_f$ | \tilde{x} | | x | |
| $a \times A$ | $q_m(1 - q_f)$ | $\frac{1}{2}\tilde{x}$ | $\frac{1}{2}\tilde{x}$ | $\frac{1}{2}x$ | $\frac{1}{2}x$ |
| $A \times a$ | $(1 - q_m)q_f$ | $\frac{1}{2}\tilde{X}$ | $\frac{1}{2}\tilde{X}$ | $\frac{1}{2}X$ | $\frac{1}{2}X$ |
| $A \times A$ | $(1 - q_m)(1 - q_f)$ | | \tilde{X} | | X |

[Fig. 2(d)].

C. Renormalization analysis

To understand the behavior in Eq. (6), let us assume that the mutation rate μ is so low that the population may have only two alleles at most, i.e., one is resident and denoted by A , and the other is mutant and denoted by a . These alleles are related to the expected progeny sex ratio but independent of the probability for the carrier to be a parent of the next generation [16]. Let x and X be the expected progeny sex ratios of a and A , respectively. The allele a is observed with frequency q_m among males and with q_f among females. The possibilities of mating events are summarized in Table I. Using this table, one can calculate the frequencies of a in the next generation as follows [11]:

$$q'_m = \frac{q_m q_f x + \frac{1}{2} q_m (1 - q_f) x + \frac{1}{2} (1 - q_m) q_f X}{q_m x + (1 - q_m) X}, \quad (7)$$

$$q'_f = \frac{q_m q_f \tilde{x} + \frac{1}{2} q_m (1 - q_f) \tilde{x} + \frac{1}{2} (1 - q_m) q_f \tilde{X}}{q_m \tilde{x} + (1 - q_m) \tilde{X}}. \quad (8)$$

For example, the expected fraction of male offspring is obtained from the last two columns as

$$\begin{aligned} r &= q_m q_f x + q_m (1 - q_f) x \\ &\quad + (1 - q_m) q_f X + (1 - q_f) (1 - q_m) X \end{aligned} \quad (9)$$

$$= q_m x + (1 - q_m) X, \quad (10)$$

which is the denominator of Eq. (7). Likewise, the probability to have male offspring with allele a is calculated from the second last column of Table I, which is the numerator of Eq. (7).

The system of Eqs. (7) and (8) has three fixed points:

$$(q_m, q_f) = (0, 0), (1, 1), (\hat{q}_m, \hat{q}_f) \quad (11)$$

where $\hat{q}_m \equiv (X - 1/2)/(X - x)$ and $\hat{q}_f \equiv 2\tilde{x}\hat{q}_m$. The first fixed point is important in the context of invasion-fixation dynamics because both q_m and q_f are small when a is newly introduced at $t = 0$. We thus linearize Eqs. (7) and (8) in the vicinity of $(q_m, q_f) = (0, 0)$ to obtain

$$\begin{pmatrix} q'_m \\ q'_f \end{pmatrix} = \frac{1}{2} \begin{pmatrix} x/X & 1 \\ \tilde{x}/\tilde{X} & 1 \end{pmatrix} \begin{pmatrix} q_m \\ q_f \end{pmatrix}. \quad (12)$$

It is straightforward to obtain the eigenvalues λ_{\pm} with $\lambda_+ \geq \lambda_-$ and the corresponding eigenvectors. The instability threshold of the fixed point $(q_m, q_f) = (0, 0)$ is characterized by $\lambda_+ = 1$. In this case, a little algebra shows

$$1 = \frac{1}{2} \left(\frac{x}{X} + \frac{\tilde{x}}{\tilde{X}} \right), \quad (13)$$

which is equivalent to Eq. (1) with $C_1 = C_2$ [11]. If $X = 1/2 + \epsilon$ with $|\epsilon| \ll 1$, then the eigenvalues are approximated to the first order of ϵ as

$$\lambda_+ \approx 1 + 2 \left(\frac{1 - 2x}{1 + 2\tilde{x}} \right) \epsilon \quad (14)$$

$$\lambda_- \approx \left(x - \frac{1}{2} \right) - 2\tilde{x} \left(\frac{1 + 2x}{1 + 2\tilde{x}} \right) \epsilon, \quad (15)$$

and the eigenvectors are

$$\vec{v}_+ \approx \left(1, 2\tilde{x} + 4\tilde{x} \left(\frac{1 + 2x}{1 + 2\tilde{x}} \right) \epsilon \right) \quad (16)$$

$$\vec{v}_- \approx \left(1, -1 - 4 \left(\frac{1 - 2x}{1 + 2\tilde{x}} \right) \epsilon \right). \quad (17)$$

If any of λ_{\pm} exceeds one, then the mutant can invade the population. It happens either when $X > 1/2$ and $x < X$, or when $X < 1/2$ and $x > X$, which implies that the sex ratio tends to 1 : 1 in agreement with Eq. (1). The linear-stability analysis can be applied to the other fixed points as well, whereby we conclude that the relevant fixed point is $(q_m, q_f) = (0, 0)$ or something close to it, as far as ϵ is sufficiently small (Fig. 3).

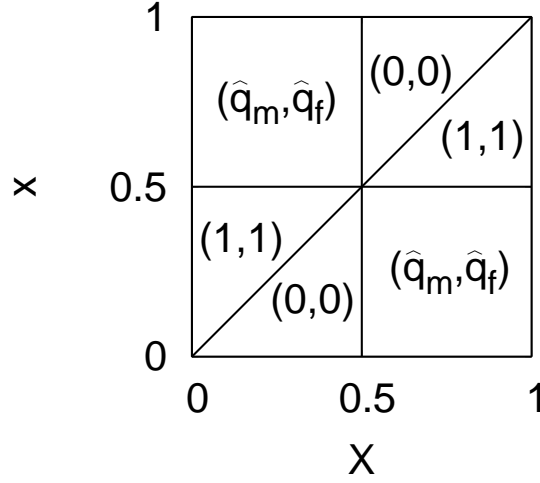


FIG. 3. Stable fixed points of Eqs. (7) and (8) represented on the (X, x) plane. For example, if $(X, x) = (0.4, 0.3)$, then the system will converge to $(q_m, q_f) = (0, 0)$.

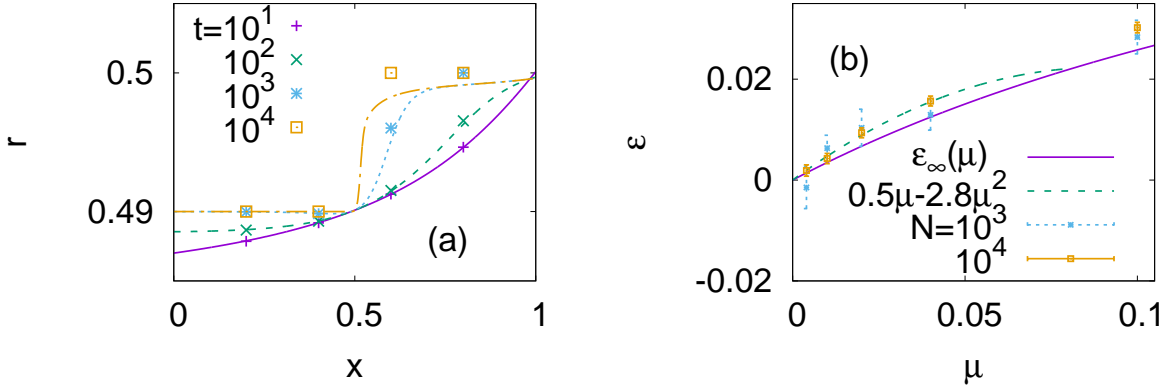


FIG. 4. (Color online) (a) Time evolution of the fraction of males [Eq. (10)] from the direct recursion [Eq. (7) and (8)] (points) and its approximation [Eq. (24)] (lines), when $q_f^{(t=t_0)} = q_m^{(t=t_0)} = 0.01$ and $X = 0.49$ in the haploid model with two alleles. (b) Deviation from the Fisherian ratio as a function of μ . The solid line shows the approximation in Eq. (32). For comparison, we also plot $0.5\mu - 2.8\mu^2$ of Eq. (6). The points with error bars show results from the Monte Carlo version of the haploid model with population size N . The errors are estimated over 50 equilibrated samples.

When a small number of mutants have appeared, (q_m, q_f) will be aligned along $\vec{v}_+ \approx (1, 2\tilde{x})$ by the fast dynamics with a timescale of $t_0 \equiv |\ln \lambda_-|^{-1} \sim O(1)$. Because $\vec{v}_- \approx (1, -1)$,

the sum of q_m and q_f is approximately conserved during this alignment, after which

$$\left(q_m^{(t=t_0)}, q_f^{(t=t_0)}\right) \approx Q \left(\frac{1}{1+2\tilde{x}}, \frac{2\tilde{x}}{1+2\tilde{x}}\right), \quad (18)$$

where $Q \equiv q_m^{(t=0)} + q_f^{(t=0)}$ is the initial fraction of mutants. The system then slowly approaches the fixed point $(0, 0)$, which means that the mutants go extinct. From the fact that $\lambda_+ \approx 1$, we see that the characteristic timescale diverges in this slow dynamics. To be more precise, the trajectory can be expressed by

$$q_f \approx \left[2\tilde{x} + 4\tilde{x} \left(\frac{1+2x}{1+2\tilde{x}}\right) \epsilon\right] q_m + C q_m^2, \quad (19)$$

with

$$C \approx -\frac{2\tilde{x}(1-2x)(1+2x)}{1+2\tilde{x}} - \frac{4\tilde{x}(21-78x+180x^2-168x^3+32x^4)}{(1+2\tilde{x})^3} \epsilon \quad (20)$$

to the order of ϵ . Note that we have to keep the order of q_m^2 . Plugging Eqs. (19) and (20) into Eq. (7) and using the continuous-time approximation, we get the following differential equation:

$$\frac{dq_m}{dt} \approx c_1 q_m + c_2 q_m^2, \quad (21)$$

where

$$c_1 \equiv 2 \left(\frac{1-2x}{1+2\tilde{x}}\right) \epsilon \quad (22)$$

$$c_2 \equiv -\frac{(1-2x)^2}{1+2\tilde{x}} - \frac{6(7-10x+12x^2-8x^3)}{(1-2x)^{-1}(1+2\tilde{x})^3} \epsilon. \quad (23)$$

One can readily solve Eq. (21) to find

$$q_m(t) = \frac{c_1 e^{c_1 t} q_m^{(t=t_0)}}{c_1 e^{-c_1 t_0} - c_2 (e^{c_1 t} - e^{-c_1 t_0}) q_m^{(t=t_0)}}. \quad (24)$$

In the limit of $\epsilon \rightarrow 0$, the timescale of this dynamics diverges because $q_m(t) \sim t^{-1}$. In addition, if $c_1 > 0$, Eq. (24) converges to

$$\lim_{t \rightarrow \infty} q_m(t) = -c_1/c_2 \approx 2\epsilon/(1-2x), \quad (25)$$

which coincides with the correct result, \hat{q}_m in Eq. (11), to the order of ϵ . Now, we have an approximate expression for the male fraction as a function of time by substituting Eq. (24)

into Eq. (10). It may be written as $r(t|X, x)$ to emphasize that it is also conditioned by X and x . Although this result involves uncontrolled approximations such as Eq. (18) and $t_0 \approx 0$, the formula works reasonably well as shown in Fig. 4(a).

Now imagine that the population initially had $X = X_0$. Random mutation occurs with a timescale $t \sim O(\mu^{-1})$ at any point of the population, and the sex ratio will be renormalized as a response to mutation as follows:

$$\epsilon_{k+1} = \int_0^1 r(t = \mu^{-1}|X = X_k, x) dx - \frac{1}{2} \quad (26)$$

$$= \int_0^1 [\epsilon_k + (x - X_k)q_m(t = \mu^{-1}|X_k, x)] dx \quad (27)$$

$$\equiv E(\epsilon_k, \mu), \quad (28)$$

where we have defined $\epsilon_k \equiv X_k - 1/2$ with an integer index $k = 0, 1, \dots$. As an example, assume that μ can be made arbitrarily small to satisfy $\mu \ll |c_1|$ all the time. According to the approximate expression given above, as $t \rightarrow \infty$, the male fraction r converges to $\epsilon_k + 1/2$ when $c_1 > 0$, and to $1/2 + O(\epsilon_k^2)$ otherwise [see, e.g., Fig. 4(a)]. As a result, we have approximately $\frac{1}{2} [(\epsilon_k + \frac{1}{2}) + \frac{1}{2}]$ on the right-hand side of Eq. (28), which is to be identified with $X_{k+1} = 1/2 + \epsilon_{k+1}$. The map obviously flows into $\epsilon_\infty = 0$, and we thus conclude that the system achieves the Fisherian ratio $X = 1/2$ in this limit of $\mu \rightarrow 0$. Having observed this limiting case, we assume that the right-hand side of Eq. (28) can still be approximated by a linear function of ϵ_k for finite μ , i.e.,

$$E(\epsilon_k, \mu) \approx U(\mu)\epsilon_k + V(\mu) \quad (29)$$

when $\epsilon_k \ll 1$. If this assumption holds, then we have

$$\epsilon_k = U^k(\mu)\epsilon_0 + \sum_{l=0}^{k-1} U^l(\mu)V(\mu), \quad (30)$$

and the ‘‘dressed’’ value converges to

$$\epsilon_\infty(\mu) = \frac{V(\mu)}{1 - U(\mu)} \quad (31)$$

as long as $|U(\mu)| < 1$. From Eq. (29), we may write $V(\mu) = \lim_{\epsilon_k \rightarrow 0} E(\epsilon_k, \mu)$ and $U(\mu) = \partial E / \partial \epsilon_k|_{\epsilon_k=0}$, both of which give closed-form expressions if the integral and the limiting process of $\epsilon_k \rightarrow 0$ commute with each other (see Appendix B for details). Then, we take another limit of $Q \rightarrow 0$ and get our main result,

$$\epsilon_\infty(\mu) \approx \frac{3\mu(\ln 3 - 1)}{14 - 12 \ln 3 + 3\mu \ln 3}, \quad (32)$$

which gives $\epsilon_\infty(\mu) \approx 0.36\mu - 1.46\mu^2$ for $\mu \ll 1$. Note the order of the limiting processes: If we had taken this zero- Q limit from the beginning, then the result would have been trivially zero. In Fig. 4(b), we see that Eq. (32) correctly captures the qualitative behavior of the Monte Carlo results.

III. DISCUSSION

We have investigated a model designed to support Fisher's theory, and it turns out that a small correction $\propto \mu$ has to be added. The reason for this correction is that the system reacts differently to female-biasing and male-biasing mutants, as already implied in Eq. (18): When $X \approx 1/2$, if we compare female-biasing mutants, say, with $x = 0.4$, and male-biasing ones with $x = 0.6$, then q_m will be greater in the latter case. On average, therefore, the male fraction is likely to be experienced as greater than $1/2$. Recall that the asymmetric part of the model is the father's predominance in determining the offspring's sex. We have shown that the system nevertheless becomes symmetric in a limit of $\mu \rightarrow 0$, which is the message of the fixed-point analysis in Eq. (13). In this sense, Fisher's theory can be thought of as a symmetry preservation mechanism. At the same time, each individual has an internal variable, the expected progeny ratio x . An interesting point is that this internal variable experiences little selection pressure when the sex ratio is 1:1, so that the gene pool can retain a high degree of genetic diversity [see, e.g., Fig. 2(c)].

For many species with female-biased sex ratios, the bias has been successfully explained within the Darwinian framework, e.g., by local mate competition [6]. On the other hand, the human sex ratio is slightly biased toward males [17], which is also believed to have an evolutionary origin. We have already seen how the Fisherian mechanism maintains an (almost) equal sex ratio at birth. If we furthermore assume that males have a higher mortality rate than females in their youth [18], then Fisher's equal-investment theory predicts a male-biased sex ratio at birth: Otherwise, the overall investment in male offspring would eventually become smaller than in female ones [6]. Unfortunately, empirical verification of this prediction is exceedingly complicated by the difficulty of measuring parental investment [19]. This work has proposed another mechanism that induces a male-biased sex ratio. In case of diploid organisms like humans, the proportionality coefficient in front of μ will depend on the dominance between the resident and mutant alleles, but it is plausible that

our estimate from the haploid model sets an upper bound for it because a recessive mutant would not much perturb the system. If we naively guess that our mechanism is responsible for the commonly known human sex ratio $\approx 1.07 : 1$ at birth, then the effective mutation rate will be $\mu \gtrsim 0.05$, meaning that the allele of the expected progeny sex ratio will be mutated roughly in 20 generations. We also note that one can empirically measure the correlation of offspring sex ratios in families, as we have depicted in Fig. 1(b). After suitable modification of the modeling assumptions, this sort of Monte Carlo calculation may be compared with genealogical data to estimate μ . One can also monitor how the sex ratio varies when mutations are induced by chemicals or radiation. For example, the human mutation rate showed a twofold increase among individuals involved in the Chernobyl accident even at a conservative estimate [20]. A recent investigation demonstrates that the sex ratio increased after the accident [21], which seems consistent with our study.

In a more general context, our study suggests that the conventional fixed-point analysis, focusing on a static equilibrium, may not catch the exact picture if perturbative effects are not taken into account, and that the behavior can be explained by renormalizing the fluctuations around the fixed point. Our result can also be regarded as an example of mutation-selection balance [22], in which selection drives the system to the fixed point while at the same time it is prevented by mutation from reaching it. Although the mutation rate is very small, its effect is of an observable magnitude because the approach to the fixed point has a diverging timescale.

IV. SUMMARY

To summarize, we have presented a detailed analysis of the haploid model, a microscopic foundation of Fisher's theory of equal investment: Although the invasion-fixation dynamics of the haploid model explains the $1 : 1$ ratio in the limit of $\mu \rightarrow 0$, the system reaches a dynamic equilibrium away from the Fisherian ratio as long as μ is nonzero. We have demonstrated this mutation-induced bias with three different approaches, i.e., Monte Carlo simulation, integrodifference equations, and renormalization analysis. All of these approaches give consistent results, revealing nontrivial dynamical aspects of the Fisherian mechanism. By linking the mutation rate and sex-ratio bias, this picture yields testable predictions, whereby the size of this effect can be assessed empirically.

Appendix A: Stationary solution of the integrodifference equations

Let us expand the stationary distributions $\phi_{\text{st}}^m(x) \equiv \phi^m(x, t \rightarrow \infty)$ and $\phi_{\text{st}}^f(x) \equiv \phi^f(x, t \rightarrow \infty)$ to the quadratic order:

$$\phi_{\text{st}}^m(x) \approx \alpha_0 + \alpha_1 x + \alpha_2 x^2 \quad (\text{A1})$$

$$\phi_{\text{st}}^f(x) \approx \beta_0 + \beta_1 x + \beta_2 x^2. \quad (\text{A2})$$

Within this approximation, we actually have 5 degrees of freedom because of the following constraint:

$$\int_0^1 [\phi_{\text{st}}^m(x) + \phi_{\text{st}}^f(x)] dx = \alpha_0 + \frac{1}{2}\alpha_1 + \frac{1}{3}\alpha_2 + \beta_0 + \frac{1}{2}\beta_1 + \frac{1}{3}\beta_2 = 1. \quad (\text{A3})$$

Let us plug Eqs. (A1) and (A2) into Eqs. (4) and (5). We define

$$S(x) \equiv \alpha_0 + \alpha_1 x + \alpha_2 x^2 - \left\{ \mu \left(\frac{\frac{\alpha_0}{2} + \frac{\alpha_1}{3} + \frac{\alpha_2}{4}}{\alpha_0 + \frac{\alpha_1}{2} + \frac{\alpha_2}{3}} \right) + \frac{1}{2}(1 - \mu) \left[\frac{x(\alpha_0 + \alpha_1 x + \alpha_2 x^2)}{\alpha_0 + \frac{\alpha_1}{2} + \frac{\alpha_2}{3}} \right. \right. \\ \left. \left. + \left(\frac{\frac{\alpha_0}{2} + \frac{\alpha_1}{3} + \frac{\alpha_2}{4}}{\alpha_0 + \frac{\alpha_1}{2} + \frac{\alpha_2}{3}} \right) \left(\frac{\beta_0 + \beta_1 x + \beta_2 x^2}{1 - \alpha_0 - \frac{\alpha_1}{2} - \frac{\alpha_2}{3}} \right) \right] \right\} \quad (\text{A4})$$

$$T(x) \equiv \beta_0 + \beta_1 x + \beta_2 x^2 - \left\{ \mu \left(1 - \frac{\frac{\alpha_0}{2} + \frac{\alpha_1}{3} + \frac{\alpha_2}{4}}{\alpha_0 + \frac{\alpha_1}{2} + \frac{\alpha_2}{3}} \right) + \frac{1}{2}(1 - \mu) \left[\frac{(1 - x)(\alpha_0 + \alpha_1 x + \alpha_2 x^2)}{\alpha_0 + \frac{\alpha_1}{2} + \frac{\alpha_2}{3}} \right. \right. \\ \left. \left. + \left(1 - \frac{\frac{\alpha_0}{2} + \frac{\alpha_1}{3} + \frac{\alpha_2}{4}}{\alpha_0 + \frac{\alpha_1}{2} + \frac{\alpha_2}{3}} \right) \left(\frac{\beta_0 + \beta_1 x + \beta_2 x^2}{1 - \alpha_0 - \frac{\alpha_1}{2} - \frac{\alpha_2}{3}} \right) \right] \right\}. \quad (\text{A5})$$

Equations (4) and (5) mean that $S(x) = T(x) = 0$, which will be only approximately true because Eqs. (A1) and (A2) are not exact. We instead minimize

$$W \equiv \int_0^1 dx [S^2(x) + T^2(x)] \quad (\text{A6})$$

with respect to $\alpha_0, \alpha_1, \alpha_2, \beta_1$ and β_2 . When $\mu = 10^{-3}$, the minimum $W_{\text{min}} = 3.46448 \times 10^{-16}$ is found at $\alpha_0 = 0.499004$, $\alpha_1 = 0.00298505$, $\alpha_2 = 2.76624 \times 10^{-10}$, $\beta_1 = -0.989074$, and $\beta_2 = -0.0059523$ [23], which indeed describe the stationary solution with high precision (Fig. 5).

Appendix B: Evaluation of $U(\mu)$ and $V(\mu)$

Let us express Eq. (28) as an integral by plugging Eq. (24) into Eq. (27). Then, we introduce $U(\mu)$ and $V(\mu)$ as in Eq. (29), which implies that $V(\mu) = \lim_{\epsilon_k \rightarrow 0} E(\epsilon_k, \mu)$ and

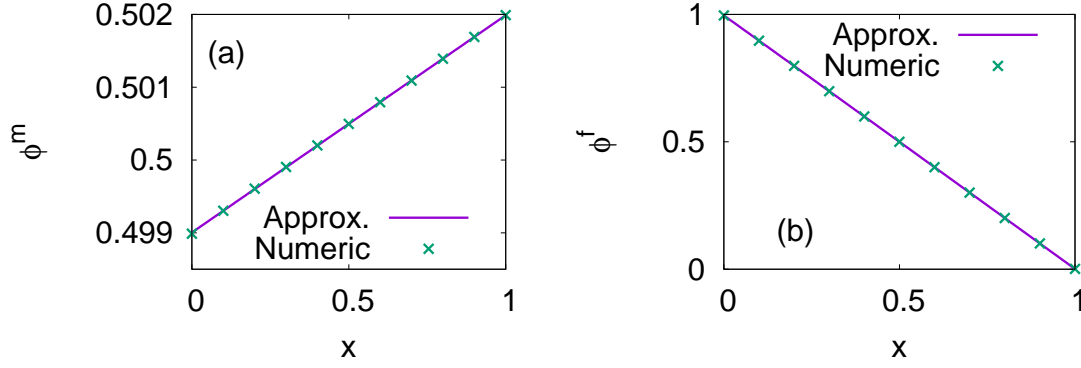


FIG. 5. (Color online) (a) Stationary probability density of being males with expected progeny sex ratio x , and (b) that of being females. The points are obtained by numerical iteration of Eqs. (4) and (5) with the same parameters as in Fig. 2(a), and the lines are drawn with the parameters that minimize Eq. (A6).

$U(\mu) = \partial E / \partial \epsilon_k |_{\epsilon_k=0}$. Provided that the integral and the limiting process of $\epsilon_k \rightarrow 0$ commute, we can find their closed-form expressions as follows [23]:

$$V(\mu) = E(0, \mu) \tag{B1}$$

$$= - \int_0^1 \frac{\mu Q (-3 + 2x)(-1 + 2x)}{2[Q(1 - 2x)^2 + \mu(3 - 2x)^2]} \tag{B2}$$

$$= - \frac{\mu Q}{4(\mu + Q)} \times \left[-2(\mu + Q) + 4\sqrt{\mu Q} \left\{ \arctan \left(\frac{3\mu + Q}{2\sqrt{\mu Q}} \right) - \arctan \left(\frac{\mu - Q}{2\sqrt{\mu Q}} \right) \right\} - (\mu + Q) \left(\ln(\mu + Q) + \ln(9\mu + Q) \right) \right], \tag{B3}$$

$$U(\mu) = \left. \frac{\partial E}{\partial \epsilon_k} \right|_{\epsilon_k=0} \quad (\text{B4})$$

$$= \int_0^1 \frac{2\mu^2(3-2x)^4(Q+2x-3)}{2(2x-3)(\mu(3-2x)^2+Q(1-2x)^2)^2} dx$$

$$+ \int_0^1 \frac{2\mu Q(1-2x)^2(2Q(12x^3-16x^2+9x-6)+(2x-3)^3)}{2(2x-3)(\mu(3-2x)^2+Q(1-2x)^2)^2} dx$$

$$+ \int_0^1 \frac{Q^2(2x-3)(1-2x)^3}{2(2x-3)(\mu(3-2x)^2+Q(1-2x)^2)^2} dx \quad (\text{B5})$$

$$= \frac{1}{4(\mu+Q)^3}$$

$$\times \left[\frac{2(\mu^4(18-66Q)+4\mu^3(8-9Q)Q+14\mu Q^3+Q^4+3\mu^2 Q^2(9+10Q))}{9\mu+Q} \right.$$

$$- \sqrt{\mu Q}(15\mu^3+Q^2(1+Q)+\mu Q(6+5Q)+\mu^2(-3+67Q))$$

$$\times \left\{ \arctan\left(\frac{\mu-Q}{2\sqrt{\mu Q}}\right) - \arctan\left(\frac{3\mu+Q}{2\sqrt{\mu Q}}\right) \right\}$$

$$- \mu \left(12(\mu+Q)^3 \ln 3 + (6\mu^3+17\mu^2 Q+2\mu(2-7Q)Q-Q^3) \right.$$

$$\left. \times (\ln(\mu+Q) - \ln(9\mu+Q)) \right) \Bigg]. \quad (\text{B6})$$

We then combine these formulas as in Eq. (31) and take another limit of $Q \rightarrow 0$ to obtain Eq. (32).

ACKNOWLEDGMENTS

H.C.J. was supported by Basic Science Research Program through the National Research Foundation of Korea (NRF) funded by the Ministry of Education (Grant No. NRF-2015R1D1A1A01058317). S.K.B. was supported by Basic Science Research Program through the National Research Foundation of Korea (NRF) funded by the Ministry of Science, ICT and Future Planning (Grant No. NRF-2017R1A1A1A05001482).

[1] W. H. James, *Hum. Biol.* **59**, 721 (1987).

[2] R. A. Fisher, *The Genetical Theory of Natural Selection* (Clarendon Press, Oxford, 1930).

- [3] R. F. Shaw and J. D. Mohler, *Am. Nat.* **87**, 337 (1953).
- [4] D. J. Rankin, K. Bargum, and H. Kokko, *Trends Ecol. Evol.* **22**, 643 (2007).
- [5] W. H. James, *J. Endocrinol.* **198**, 3 (2008).
- [6] S. West, *Sex Allocation* (Princeton University Press, Princeton, NJ, 2009).
- [7] W. A. Kolman, *Am. Nat.* **94**, 373 (1960); J. Verner, *ibid.* **99**, 419 (1965); P. D. Taylor and A. Sauer, *ibid.* **116**, 305 (1980).
- [8] I. Eshel, *Heredity* **34**, 351 (1975).
- [9] E. L. Charnov, *The Theory of Sex Allocation* (Princeton University Press, Princeton, NJ, 1982).
- [10] S. Karlin and S. Lessard, *Theoretical Studies on Sex Ratio Evolution* (Princeton University Press, Princeton, NJ, 1986).
- [11] J. Seger and J. W. Stubblefield, “Models of sex ratio evolution,” in *Sex Ratios: Concepts and Research Methods*, edited by I. C. W. Hardy (Cambridge University Press, New York, 2002) pp. 2–25.
- [12] D. Trichopoulos, *Hum. Biol.* **39**, 170 (1967).
- [13] M. J. Khoury, J. D. Erickson, and L. M. James, *Am. J. Hum. Genet.* **36**, 1103 (1984).
- [14] C. Gellatly, *Evol. Biol.* **36**, 190 (2009).
- [15] M. E. J. Newman, *Computational Physics* (CreateSpace Independent, San Bernardino, CA, 2013).
- [16] D. L. Hartl, *A Primer of Population Genetics* (Sinauer Associates, Inc., Sunderland, MA, 1981) p. 144.
- [17] The World Bank, <https://databank.worldbank.org/data/source/gender-statistics>.
- [18] S. Stinson, *Am. J. Phys. Anthropol.* **28**, 123 (1985).
- [19] D. F. Sieff, L. Betzig, L. Cronk, A. G. Fix, M. Flinn, L. Sattenspiel, K. Gibson, D. A. Herring, N. Howell, S. R. Johansson, *et al.*, *Curr. Anthropol.* **31**, 25 (1990).
- [20] Y. E. Dubrova, V. N. Nesterov, N. G. Krouchinsky, V. A. Ostapenko, R. Neumann, D. L. Neil, and A. J. Jeffreys, *Nature* **380**, 683 (1996); H. S. Weinberg, A. Korol, V. Kirzhner, A. Avivi, T. Fahima, E. Nevo, S. Shapiro, G. Rennert, O. Piatak, E. Stepanova, *et al.*, *Proc. Royal Soc. B* **268**, 1001 (2001); A. P. Møller and T. A. Mousseau, *Trends Ecol. Evol.* **21**, 200 (2006).
- [21] H. Scherb, R. Kusmierz, and K. Voigt, *Environ. Health* **12**, 63 (2013).

- [22] F. Bertels, C. S. Gokhale, and A. Traulsen, *Genetics* **206**, 2149 (2017).
- [23] “Mathematica, Version 9.0,” (Wolfram Research, Inc., Champaign, IL, 2012).